Amorphization Mechanism of Icosahedral Metal Nanoclusters

E. Aprà,[1] F. Baletto,[2] R. Ferrando,[3] and A. Fortunelli[4,*]

[1]*William R. Wiley Environmental Molecular Sciences Laboratory, Pacific Northwest National Laboratory, Richland, Washington 99352, USA*

[2]*ICTP, Strada Costiera 11, 34014, Trieste, Italy*

[3]*INFM and IMEM-CNR, Dipartimento di Fisica dell'Università di Genova, via Dodecaneso 33, 16146 Genova, Italy*

[4]*Molecular Modeling Laboratory, Istituto per i Processi Chimico-Fisici (IPCF) del CNR, Via G. Moruzzi 1, 56124, Pisa, Italy*

(Received 4 March 2004; published 4 August 2004)

The amorphization mechanism of icosahedral Pt nanoclusters is investigated by a combination of molecular dynamics simulations and density functional calculations. A general mechanism for amorphization, involving rosettelike structural transformations at fivefold vertices, is proposed. In the rosette, a fivefold vertex is transformed into a hexagonal ring. We show that, for icosahedral Pt nanoclusters, this transformation is associated with an energy gain, so that their most favorable structures have a low symmetry even at icosahedral magic numbers, and that the same mechanism underlies the formation of amorphous structures in gold.

DOI: 10.1103/PhysRevLett.93.065502 PACS numbers: 61.46.+w

Clusters of transition and noble metals are interesting for their physical and chemical properties, and for technological applications [1]. In this context, platinum clusters are of great importance because of their role in many catalytic processes [2]. The starting point for understanding cluster properties is the determination of their structure, which is usually a nontrivial task, since clusters can assume a wide variety of structures. The simplest ones are pieces of the bulk crystal lattice, which is fcc for noble metals and Pt. Clusters can present also noncrystalline structures, such as icosahedra (Ih) and decahedra (Dh) [3], having fivefold symmetries. Interatomic distances in Ih and Dh differ with respect to the ideal bulk value, thus giving a volume contribution to the energy that is absent in fcc clusters. This volume contribution may be compensated by a lower surface energy: especially Ih structures, which present a close-packed surface and a low surface/volume ratio, can be more favorable than fcc structures at small sizes, where surface contributions to the energy are dominant. All these structures can be of special energetic stability at the so-called structural *magic numbers,* which are the numbers of atoms N needed to complete a perfect cluster of a given symmetry. For example, at $N = 13$ and 55 perfect Ih, truncated Dh, and fcc cuboctahedra (Oh) are obtained [3]. Several different calculations indicate that nickel, copper, and silver clusters adopt preferentially the Ih structure at $N = 55$ [4–6]. On the contrary, calculations on gold clusters show a preference for low-symmetry structures [7]. The latter are often called amorphous because their radial distribution functions resemble those of liquid clusters. These findings have been rationalized in terms of the bond order–bond length correlation in metallic systems [8,9]. In Au, bonds have a much stronger tendency to contract with decreasing coordination than in Ag, Cu, or Ni, and this favors the disordering of the cluster surface. From this point of view, Pt is intermediate between Au and Ag, and its behavior with respect to amorphization is still an open problem (see references to experimental controversy in [10]).

In this Letter we show that icosahedral Pt clusters have indeed a tendency towards amorphization, namely, to present low-symmetry structures at magic sizes. We propose a general amorphization mechanism of Ih clusters, which involves the formation of *rosettelike* structural excitations at the fivefold vertices. This mechanism also underlies the formation of amorphous clusters in Au. In the first step of our procedure we describe Pt by a many-body atom-atom potential (developed by Rosato, Guillopé, and Legrand (RGL) [11]; form and parameters are given in Ref. [6]) and perform a global minimum search by quenching $\sim 10^6$ snapshots from high-temperature molecular dynamics simulations. The results are checked by a genetic algorithm global optimization. In this way we are able to collect a huge catalog of minima, comprising hopefully the global minimum and all other low-lying minima. In the second part of the procedure, we locally optimize the most significant structures by density functional theory (DFT) calculations. These are carried out with the DFT module of the NWCHEM package [12], and use the Becke functional [13] for exchange and the Perdew-Wang functional [14] for correlation, a $(7s5p5d)/[6s3p2d]$ Gaussian-type-orbital basis set [15], and an effective core potential [16] incorporating spin-orbit averaged relativistic effects for the platinum atom. More details can be found in [10,17].

The global optimization results for Pt_{55} using the RGL potential indicate that the lowest minimum is an icosahedron (Ih_{55}; see Fig. 1). Oh and truncated Dh structures lie at higher energy, in agreement with DFT calculations [10]. Among the other low-lying minima, we single out a very peculiar structure, which is referred to as the *rosette*

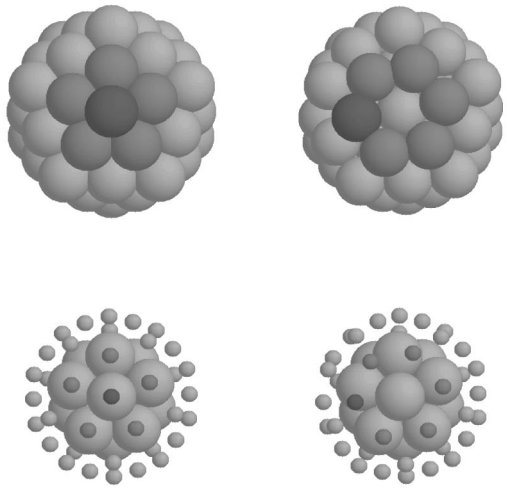

FIG. 1. Ih_{55} (left column) and rosette (right column) structures, as obtained within the RGL description. In the bottom row, the atoms of the external shell are represented with small spheres to show the 13 atoms forming the cluster core. The rosette is obtained from the Ih_{55} by displacing a vertex atom (dark gray) to form a hexagonal ring together with its five neighbors of the Ih_{55} surface.

in the following. The rosette is an elementary transformation of the Ih_{55} taking place at a single fivefold vertex. As shown in Fig. 1, a vertex atom is pushed out and inserted between its five neighbors on the surface, to form a sixfold ring centered around the original position of the vertex. This transformation breaks the Ih symmetry. However, the shell structure of the Ih is preserved in the rosette, which still has an inner core of 13 atoms—a somewhat distorted Ih_{13}—surrounded by an outer shell of 42 atoms, exactly as in the Ih_{55}. According to the RGL potential, the rosette is higher in energy than the Ih_{55} by $\Delta E = E^{\mathrm{ros}} - E^{\mathrm{Ih}} \sim 0.5$ eV, as shown in Table I.

What factors favor the rosette? We can try to give an answer by comparing the atomic energies E_i in the rosette and the Ih_{55}. In the rosette, the atoms of the outer shell have higher energies than in the Ih_{55}, whereas the opposite holds for the atoms of the inner core. Putting $E_{\mathrm{shell}}, E_{\mathrm{core}} = \sum_i E_i$, with i running on the 42 shell and the 13 core atoms, respectively, we find that $\Delta E_{\mathrm{shell}} = E^{\mathrm{ros}}_{\mathrm{shell}} - E^{\mathrm{Ih}}_{\mathrm{shell}} > 0$, whereas $\Delta E_{\mathrm{core}} = E^{\mathrm{ros}}_{\mathrm{core}} - E^{\mathrm{Ih}}_{\mathrm{core}} < 0$. This behavior is due to the peculiar interplay between the bond order–bond length correlation in metallic systems and the geometry of the Ih structure. In fact, highly coordinated atoms prefer larger first-neighbor distances than atoms with low coordination. Therefore, inner atoms would prefer to have neighbors at the ideal distance of the bulk fcc crystal, while surface atoms would better have contracted bonds. This is contrary of what happens in an Ih structure, where inner bonds are more compressed than surface bonds. In the rosette structure the surface is rearranged in such a way that there are fewer bonds than in the Ih_{55}, but these bonds are shorter on average. Moreover, the inner core is expanded, and its atoms are less compressed than in the Ih_{55}. The final result is that inner atoms lower their energy at the expense of surface atoms. Depending on the metal, the gain may either compensate the loss or not. As shown in Table I, for Ag, Pd, and Pt, the gain does not compensate the loss within the RGL description, but for Au the opposite happens, and the rosette is lower in energy than the Ih_{55}. The energy gain of core atoms can be rationalized using the concept of interaction *stickiness* [18]. A sticky potential is characterized by a high energetic penalty for changing the interatomic distances from their ideal bulk value. In a sticky metal, the highly coordinated core atoms gain more energy from the core expansion of the transformation $Ih_{55} \rightarrow$ rosette. Moreover, the rearrangement of the surface is less disadvantageous for systems with stronger bond contraction at decreasing coordination [8] because they present a weaker dependence of the energy on the number of bonds. This completely agrees with the normalized energy changes of shell and core atoms in Table I, since noble and quasinoble metals can be ordered with increasing stickiness and tendency to bond contraction as follows [6]: Ni, Cu, Ag, Pd, Pt, Au (with Pd and Pt essentially at the same level of stickiness). For Ni and Cu we have not succeeded in stabilizing the rosette, which probably does not even correspond to a local minimum. We have also investigated the behavior of Ih_{55} and rosette with temperature, by performing freezing and melting molecular dynamics simulations, and calculating the occupation probability of the two minima within the harmonic superposition approximation [19]. It turns out that the entropic effects favor the rosette against the Ih_{55} at temperatures above 600 K.

TABLE I. Results from the RGL potential modeling for Ih_{55} and rosette structures. Absolute energy differences (in eV) between rosette and Ih_{55} $\Delta E = E^{\mathrm{ros}} - E^{\mathrm{Ih}}$, and energy difference among external atoms $\Delta E_{\mathrm{shell}} = E^{\mathrm{ros}}_{\mathrm{shell}} - E^{\mathrm{Ih}}_{\mathrm{shell}}$ and among core atoms $\Delta E_{\mathrm{core}} = E^{\mathrm{ros}}_{\mathrm{core}} - E^{\mathrm{Ih}}_{\mathrm{core}}$. Normalized energy changes (i.e., divided by the value for the Ih_{55} structure) are also reported.

Metal	ΔE	$\Delta E/\lvert E^{\mathrm{Ih}}\rvert$	$\Delta E_{\mathrm{shell}}$	$\Delta E_{\mathrm{shell}}/\lvert E^{\mathrm{Ih}}_{\mathrm{shell}}\rvert$	ΔE_{core}	$\Delta E_{\mathrm{core}}/\lvert E^{\mathrm{Ih}}_{\mathrm{core}}\rvert$
Ag	0.584	4.10×10^{-3}	0.997	9.5×10^{-3}	−0.413	-1.11×10^{-2}
Pd	0.449	2.34×10^{-3}	1.139	8.0×10^{-3}	−0.690	-1.42×10^{-2}
Pt	0.483	1.66×10^{-3}	1.550	7.1×10^{-3}	−1.067	-1.46×10^{-2}
Au	−0.309	-1.59×10^{-3}	0.823	5.4×10^{-3}	−1.132	-2.38×10^{-2}

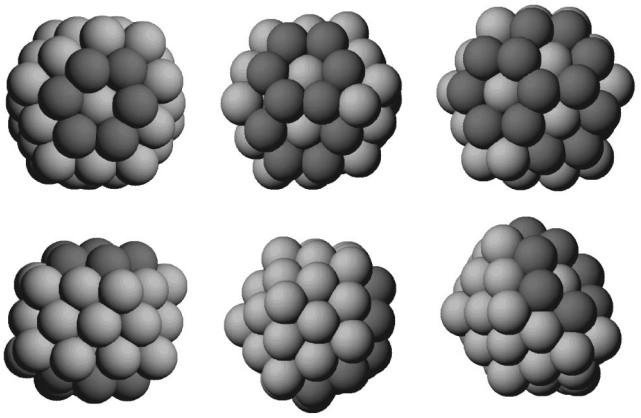

FIG. 2. From left to right, front (top row) and side (bottom row) views of the double opposite rosette (dor), of the double paired rosette (dpr), and of the triple rosette (tr), as obtained within the RGL description. Atoms belonging to the hexagonal rosette rings are depicted in darker gray.

An interesting question is whether the introduction of further rosette motifs on the surface can be energetically favorable. We thus investigate three multiple-rosette structures within the RGL description (see Fig. 2): the double opposite rosette (dor) with two rosettes at opposite fivefold vertices, the double paired rosette (dpr) with two rosettes at nearby fivefold vertices, and the triple rosette (tr) with three rosettes at nearby vertices. The energy differences of these structures with respect to the single rosette are given in Table II. For Au, the dpr structure is better than the single-rosette, and the tr structure is even lower in energy. Our global optimization confirms that these structures are the lowest-energy amorphous structures for Au clusters, in agreement with the findings in [5,7], thus showing that the amorphization mechanism of Au clusters occurs through *the generation of multiple rosettes*. In the case of Ag and Pd, multiple rosettes are always higher in energy than the single rosette. Platinum is in between, since the dpr structure is slightly better than the single rosette, while the tr structure is slightly worse. In all metals, rosettes at opposite vertices are always unfavorable (in Ag they are not even a stable local minimum). In summary, multiple rosettes are clearly favorable in Au, and unfavorable in Ag and Pd. The case of Pt is less clear.

TABLE II. Results from the RGL potential modeling for multiple-rosette structures. E^{ros}, E^{dor}, E^{dpr}, and E^{tr} are the energies of single rosette, double opposite rosette, double paired rosette, and triple rosette, respectively.

Metal	$E^{\mathrm{dor}} - E^{\mathrm{ros}}$	$E^{\mathrm{dpr}} - E^{\mathrm{ros}}$	$E^{\mathrm{tr}} - E^{\mathrm{ros}}$
Ag	⋯	0.206	0.453
Pd	0.910	0.017	0.155
Pt	1.743	−0.059	0.065
Au	0.640	−0.226	−0.329

The conclusion, within the RGL description, is that—apart from Au—the best candidate for amorphization is Pt, because it has the smallest relative energy difference between rosette and Ih_{55} (see Table I), and because in Pt multiple rosettes are as favorable as the single rosette. At the RGL level, Pt clusters are not amorphous. However, this description is approximate, as it does not take into account some features of bonding, such as its directionality, which play an important role in Pt [20]. Therefore, more accurate modeling is needed, and in the following we analyze both Ih_{55} and rosette clusters by DFT calculations.

To start, we optimize locally the symmetrical structures considered in [10]: Ih_{55}, Oh_{55}, and Dh_{55}, but removing any symmetry constraints. At variance with the Pt_{13} case, we do not find any significant symmetry breaking, and the relaxation energy is negligible, less than 0.1 eV, with the energy order ($Ih < Dh < Oh$) still holding. Quite different results are obtained from the local optimization of the RGL single-rosette structure: the energy drops below that of the Ih_{55} by more than 1.6 eV, and the structure undergoes a substantial rearrangement, finally producing the optimized configuration displayed in Fig. 3. The Ih arrangement is thus *metastable* at the DFT level with respect to the rosette deformation of one of its vertices. A possible explanation of the difference with respect to the RGL results follows from a comparison between the optimized RGL and DFT rosette structures of Figs. 1 and 3. It can be clearly seen that the rosette is conserved by the DFT optimization, but also that the atom at the center of the rosette, which lies well

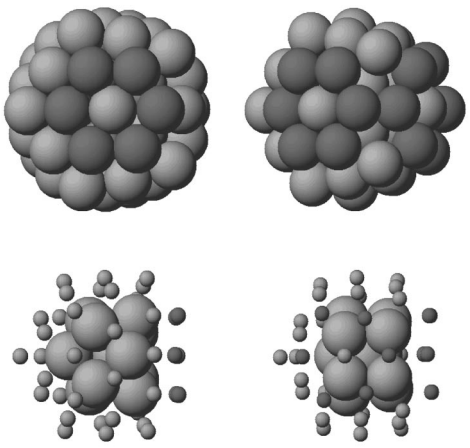

FIG. 3. Front (top row) and side (bottom row) views of the rosette (left) and double rosette (right) structures after DFT relaxation. In the side views, external atoms are represented by small spheres to show the inner part of the cluster. There are 12 and 11 internal atoms in the rosette and double rosette, respectively. Atoms belonging to the hexagonal rosette rings are depicted in darker gray.

inside the cluster in Fig. 1, *moves upward to the surface* in Fig. 3, thus producing what is essentially the typical seven-atom face of a (111) plane of a fcc crystal. The reason why the RGL potential misses this structural rearrangement cannot be due to an incorrect choice of the parameters, as it apparently derives from *anisotropic* or *bond directionality* [20] effects. Platinum, in fact, is a third-row metal, in which the relativistic contraction of the *s*-orbital brings it to substantially overlap with the *d* orbitals, decreasing the localized character of the latter and strongly increasing their contribution to chemical bonding [21]: see, for example, Ref. [20], in which this effect is discussed within the first-principles derivation of tight-binding parameters. This is in agreement with the ease of hex reconstruction formation on extended Au and Pt surfaces (at variance with, say, Pd and Ag surfaces). In passing, we note the quenching of the electron spin of the cluster: from $S = 6$ in the Ih_{55} to $S = 1$ in the ground state of the rosette (quasidegenerate with a $S = 0$ state). The gap in the one-electron energy spectrum is small, $\leq$ 0.1 eV, and the bandwidth is comparable with that of the Oh structure.

Are multiple-rosette structures favorable in Pt at the DFT level? To answer this question, we optimize a properly chosen multiple-rosette configuration, selecting the one that in principle should be the least favorable, namely, the double opposite rosette (similar to the one shown in Fig. 2). After local DFT optimization, the structure of Fig. 3 is obtained. Two points are worth noting. First, the minimized energy of this structure lies *below* the energy of the single rosette by ≈ 0.4 eV. The platinum tendency to form the rosette motif on the surface is so strong at the DFT level that even starting from an unfavorable arrangement of two rosettes, lying on opposite sides, one still decreases the energy with respect to a single rosette. Second, one of the two rosette motifs switches place during the optimization from being symmetrically opposite to the other rosette to moving on to a nearest-neighbor vertex, as the atom at the center of the rosette becomes a vertex of a pseudo-C_5 axis, and leaves a hole in the inner shell immediately below it. These subtle effects are apparently due to long-range interactions between different parts of the cluster. The spin is again effectively quenched (the ground state has $S = 0$), and the gap in the one-electron spectrum is ≈ 0.1 eV. We note that at the DFT level the cluster core, too, suffers a much stronger rearrangement than at the semiempirical level. A substantial rearrangement of the core (but of a different type), allowing the relief of local stress, was found in Ref. [9] for Au clusters.

In conclusion, our calculations show that icosahedral Pt clusters have, indeed, a tendency towards amorphization. The amorphization mechanism, which is effective also in gold clusters and generally in metallic systems with sticky potential and strong bond order–bond length correlation, takes place through the generation of (eventually multiple) rosette motifs at the fivefold vertices. The rosette motif allows an efficient relaxation of the internal atoms, which overcomes a surface energy penalty. In the case of platinum, the driving force favoring the rosette is enhanced by bond directionality effects due to *d-d* interactions.

We acknowledge financial support from the Italian CNR for the project "(Supra-)Self-Assemblies of Transition Metal Nanoclusters" within the framework of the ESF EUROCORES SONS. A. F. acknowledges the Italian INSTM for a grant at the CINECA supercomputing center. A portion of the research described in this manuscript was performed at the W. R. Wiley EMSL, a national scientific user facility sponsored by the U.S. DOE OBER and located at PNNL. PNNL is operated for the DOE by Battelle.

*Corresponding author.
Email address: fortunelli@ipcf.cnr.it

[1] *Progress in Experimental and Theoretical Studies of Clusters*, edited by T. Kondow and F. Mafuné (World Scientific, New York, 2003).
[2] K. J. Klabunde, *Nanoscale Materials in Chemistry* (Wiley, New York, 2001).
[3] T. P. Martin, Phys. Rep. **273**, 199 (1996).
[4] D. R. Jennison, P. A. Schultz, and M. P. Sears, J. Chem. Phys. **106**, 1856 (1997).
[5] K. Michaelian, N. Rendón, and I. L. Garzón, Phys. Rev. B **60**, 2000 (1999).
[6] F. Baletto *et al.*, J. Chem. Phys. **116**, 3856 (2002).
[7] I. L. Garzon *et al.*, Phys. Rev. Lett. **81**, 1600 (1998).
[8] J. M. Soler *et al.*, Phys. Rev. B **61**, 5771 (2000).
[9] J. M. Soler, I. L. Garzón, and J. D. Joannopoulos, Solid State Commun. **117**, 621 (2001).
[10] E. Aprà and A. Fortunelli, J. Phys. Chem. A **107**, 2934 (2003).
[11] V. Rosato, M. Guillopé, and B. Legrand, Philos. Mag. A **59**, 321 (1989).
[12] R. A. Kendall *et al.*, Comput. Phys. Commun. **128**, 260 (2000).
[13] A. D. Becke, Phys. Rev. A **38**, 3098 (1988).
[14] J. P. Perdew and Y. Wang, Phys. Rev. B **33**, 8800 (1986); J. P. Perdew *et al.*, Phys. Rev. B **46**, 6671 (1992).
[15] A. Schaefer, C. Huber, and R. Ahlrichs, J. Chem. Phys. **100**, 5829 (1994).
[16] D. Andrae *et al.*, Theor. Chim. Acta **77**, 123 (1990).
[17] E. Aprà and A. Fortunelli, J. Mol. Struct., Theochem **501/502**, 251 (2000).
[18] J. P. K. Doye, D. J. Wales, and R. S. Berry, J. Chem. Phys. **103**, 4234 (1995).
[19] J. P. K. Doye and F. Calvo, Phys. Rev. Lett. **86**, 3570 (2001).
[20] A. Fortunelli and A. M. Velasco, Int. J. Quantum Chem. **99**, 654 (2004).
[21] S. Taylor *et al.*, J. Chem. Phys. **89**, 5517 (1988).